

# Scanning tunneling microscope measurements of the amplitude of vibration of a quartz crystal oscillator

B. Borovsky,<sup>a)</sup> B. L. Mason, and J. Krim

*Department of Physics, Box 8202, North Carolina State University, Raleigh, North Carolina 27695-8202*

(Received 13 March 2000; accepted for publication 23 June 2000)

We report highly accurate measurements of the vibrational amplitude of a transverse shear mode quartz resonator, obtained by directly imaging the surface oscillatory motion with a scanning tunneling microscope. Amplitude measurements, performed over a range of resonator drive levels and quality factors, agree with theoretical predictions to within a factor of two. © 2000 American Institute of Physics. [S0021-8979(00)04419-4]

## I. INTRODUCTION

Piezoelectric quartz crystals operating as high precision resonators have been employed for decades as deposition rate monitors and for frequency control purposes.<sup>1</sup> In recent years their use has increasingly been diversified to probe characteristics of bulk solids and liquids, as well as thin films and interfaces, in an extraordinarily wide range of biological, chemical, electrochemical, and physical applications.<sup>2</sup> Many of these applications require a precise knowledge of the amplitude of vibration of the resonator in order to fully explore the significance of the result.<sup>3</sup> To date, such information has been lacking. We report here a direct measurement of the amplitude of a quartz crystal oscillator vibrating in transverse shear mode, obtained by directly measuring the surface oscillatory motion with a scanning tunneling microscope. Our results represent the first highly accurate measurements of vibrational amplitude to be performed in a manner which allows direct comparison with theory.

The first thorough investigation of in-plane vibrations of a quartz oscillator was performed by Sauerbrey<sup>4</sup> in the 1960's utilizing an elegant, but complex, optical method.<sup>5</sup> Sauerbrey measured the maximum amplitude and the overall vibration pattern for many transverse shear modes, and established that the amplitude of vibration of the fundamental mode was well described by a Gaussian profile along the diameter of a quartz disk. A more direct measurement of in-plane vibration amplitudes was performed by both Gerdes and Wagner,<sup>6</sup> and Bahadur and Parshad<sup>7,8</sup> using scanning electron microscopy. Several other techniques have improved the measurement of vibration patterns and amplitude distributions, but have not allowed accurate determination of the amplitude itself.<sup>3,9,10</sup>

From classic driven oscillator theory, it is clear that to compare the values of the amplitude measured by different authors, and likewise to compare with theoretical calculations, it is essential to know both the drive voltage applied to the crystal and the quality factor,  $Q$ , of the system.<sup>11</sup> However, to date these key parameters have been reported only by Martin and Hager,<sup>3</sup> whose technique measured the amplitude distribution. In view of recent theoretical work by

Kanazawa, it is now possible to compare experimental measurements of the vibration amplitude itself to detailed calculations for quartz.<sup>12</sup> Using a physical model for the same type of quartz sample as used in our experiments, Kanazawa predicted that the average amplitude of vibration is 133 nm for a peak sinusoidal drive voltage of 1.0 V and a  $Q$  of 100 000.

## II. EXPERIMENTAL SETUP

Our experimental arrangement is shown schematically in Fig. 1. The quartz crystal oscillators employed for this study were 5 MHz fundamental mode "AT-cut" (transverse-shear mode) crystals identical to those which are routinely employed as quartz crystal microbalances. They consisted of thin disks of single crystal quartz (diameter 1 cm) with metal electrodes (diameter 0.6 cm) deposited onto each side of the disk. The crystals, with pre-existing 1000-Å-thick chromium electrodes, were mounted on a commercial scanning tunneling microscope sample holder with two points of contact. These mounting points also served as electrical connections to drive the oscillatory motion of the quartz. The sample was then introduced to a vacuum chamber which housed a commercial scanning tunneling microscope<sup>13</sup> operated by commercial control electronics.<sup>14</sup> The system was evacuated, and upon attaining a base pressure of  $2 \times 10^{-8}$  Torr, 500 Å of copper was thermally evaporated onto the electrode of the quartz oscillator upon which the scanning tunneling microscopy (STM) imaging was to be performed, so as to provide a clean and conductive surface. The STM tip consisted of etched tungsten wire and was located exactly at the center of the electrode. It is well established that the amplitude of oscillation is a maximum at this location and decays in a Gaussian manner as the distance from the center increases radially.<sup>3,4,10</sup> Typical tunneling parameters were 1–2 nA current with 200–500 mV bias. (Copper was chosen as the electrode material on account of its relevance to research which we were performing on a separate topic. The measurements described here are also performable under atmospheric conditions using relatively inert electrode metals, such as gold or nickel, and an inert tip material, such as Pt/Rh alloy).

To drive the resonance of the crystal, we employed the circuit shown in Fig. 2. In this circuit, the crystal is placed

<sup>a)</sup>Electronic mail: borovsky@unity.ncsu.edu

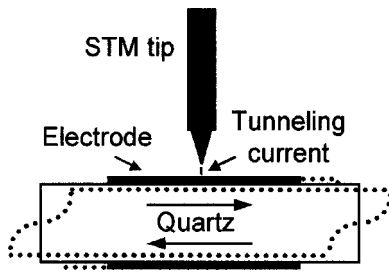


FIG. 1. A schematic diagram of our measurement technique. The STM tip scans the surface of a vibrating quartz disk, at its center, to measure the oscillation amplitude of the fundamental transverse shear mode.

parallel with an inductor and this combination is then placed in series with a resistor. The entire combination is driven by a commercial function generator.<sup>15</sup> The purpose of the capacitor,  $C=0.5 \mu\text{F}$ , is to isolate the dc STM bias voltage from ground, while acting as a short to ground at 5 MHz. The resistance value limits the drive voltage applied to the crystal, while the crystal-inductor combination is a tank circuit which allows the exchange of electrical energy between the crystal and inductor. We have chosen a resistance of  $220 \Omega$ , which typically gives a maximum peak drive voltage of 1 V across our crystals. The range of vibration amplitudes reported here is comparable to that we obtain by driving the crystal with a standard crystal oscillator circuit.<sup>16</sup> We have chosen an inductance of  $2 \mu\text{H}$ . A smaller inductor, and therefore a smaller resistive load in parallel with the crystal, improves the  $Q$  of the system while decreasing the signal-to-noise ratio.<sup>17</sup>

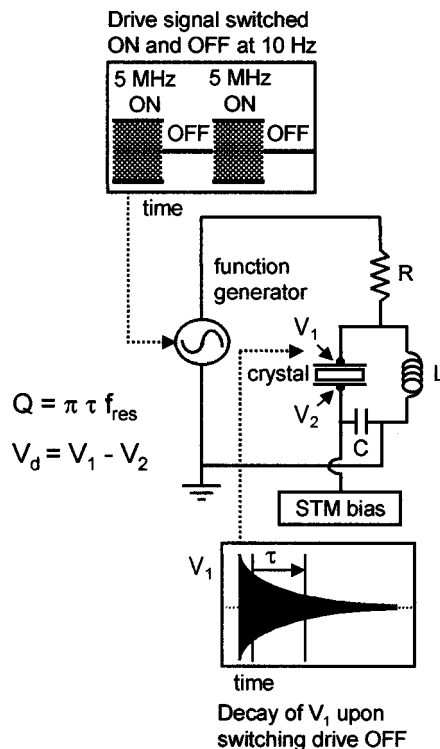


FIG. 2. A schematic diagram showing the electrical circuit used to drive the crystal and the “ring-down” technique used for measuring the quality factor, or  $Q$ , of the system.

Monitoring the voltage across the crystal-inductor combination provides a convenient way to detect the resonance and measure the  $Q$  of the system. Since the resonance of the crystal (the so-called series resonance) corresponds to a minimum in the crystal’s impedance, the resonant frequency can be found very nearly by detecting a minimum in the voltage across the crystal. We have used the “ring-down” technique of measuring  $Q$ ,<sup>17</sup> which is demonstrated in Fig. 2. By switching the drive voltage off periodically, the exponential decay of undriven oscillations may be monitored by the decaying sinusoidal voltage across the crystal. The  $Q$  of the system is given by  $\pi \tau f_{\text{res}}$ , where  $\tau$  is the exponential decay time constant for the amplitude, and  $f_{\text{res}}$  is the resonant frequency.<sup>18</sup> We checked the accuracy of our  $Q$  measurements using an independent calibration technique described elsewhere.<sup>19</sup> The drive voltage across the crystal was determined by subtracting the signals on its two electrodes,  $V_d = V_1 - V_2$ , accounting for their relative phase difference. (Herein we always report peak voltages rather than peak-to-peak). Since the crystal is located inside a vacuum chamber, its electrodes are necessarily connected to the circuit by long segments of wire. These wires sustain measurable voltage drops which must be taken into account in determining the drive voltage. Upon opening our vacuum chamber, we probed the voltages  $V_1$  and  $V_2$  at points very close to the electrodes, thereby calibrating our measurements taken outside of vacuum.<sup>20</sup> The resulting accuracy is estimated to be 10%. The two parameters,  $Q$  and  $V_d$ , essential to comparing the results to theory were thus recorded for all measurements of the drive amplitude.

### III. RESULTS

The ability to image a vibrating surface with an STM, while unexpected, may be attributed to the three widely separated time scales involved, and the exponential dependence of the tunneling current on tip–surface separation. The characteristic frequencies of the scanner (Hz), the feedback loop (kHz), and the quartz crystal (MHz) are each separated by three orders of magnitude. Conventional STM operation relies on the feedback loop being much faster than the scanner (in constant-current mode). The fact that the vibrations of our quartz substrate are in turn much faster than the feedback loop causes the tip to be held at a separation from the surface which on average (over many oscillation cycles) gives the desired tunneling current. Qualitatively, the closest approach of the surface to the tip during each cycle is weighted most heavily in this average, due to the exponential dependence of the tunneling current on separation, so the tip is held at an altitude sufficient to avoid direct contact of the tip and surface. This allows the STM tip to image the vibrating surface without crashing into it, as is evident in our images, which show very few changes in the surface topography throughout the measurement process.

Figure 3 displays a pair of images which demonstrate our measurement technique. These  $177 \text{ nm} \times 177 \text{ nm}$  images are raw data, presented without any processing. The gray-scale is proportional to the height of the surface, with bright areas higher than dark areas. Image (a) shows the stationary

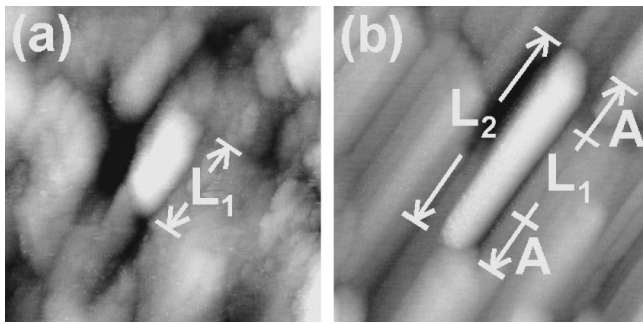


FIG. 3. A pair of  $177\text{ nm}\times 177\text{ nm}$  images demonstrating our amplitude measurement technique. The same prominent asperity is shown while the surface is stationary (a) and oscillating (b). The apparent elongation of the asperity can be used to determine the amplitude of oscillation.

crystal. A prominent asperity is visible in the center of the image. Image (b) shows the same region as the crystal oscillates at its resonant frequency with a peak drive voltage of  $0.46\text{ V}$  and a  $Q$  of  $55\,000$ . The asperity of (a) appears elongated in (b) since the entire region oscillates back and forth very rapidly along the shear direction. The effect is similar to a photograph of a moving object with a long exposure time. Measuring along the shear direction, the length of the feature in image (a) is  $L_1 = 54\text{ nm}$ . In image (b), its length is  $L_2 = 125\text{ nm}$ . The amplitude of oscillation is determined by the following equation:

$$L_2 = L_1 + 2A. \quad (1)$$

In this case, we find  $A = 36\text{ nm}$ . The uncertainty of the amplitude measurements in most cases is  $\pm 2\text{ nm}$ , estimated by determining the scatter among different data sets for the same measurement conditions. The length of a given feature in one image can typically be determined to within  $\pm 0.5\text{ nm}$ . Corrections for the overall tilt of the surface relative to the plane of the scan were found to be exceedingly small. The absolute accuracy of the amplitude measurements was ensured by calibrating our STM scanner using a commercial standard.<sup>21</sup> This standard allows lateral calibration on the length scale of  $750\text{ nm}$ , with a reported precision of  $6\%$ . Linearity of the calibration coefficients down to the  $50\text{--}100\text{ nm}$  length scale was verified using images that progressively zoom-in on a given feature of about that size.

Figure 4 presents four images which demonstrate the effectiveness and reliability of our technique. These larger scale images ( $266\text{ nm}\times 266\text{ nm}$ ) are displayed in perspective view with grayscale illumination in order to better indicate the surface topology. The vertical scale is the same as the lateral scale. Images (a) and (b) show the stationary surface before and after, respectively, a long series of images of the oscillating surface. Images (c) and (d) show the oscillating surface at two different peak drive voltages,  $0.23$  and  $0.93\text{ V}$ , respectively. The  $Q$  value is  $54\,000$ . The black cross marks the same feature in all four images. [There is an overall shift in location between images (a) and (b). This is the result of thermal drift due to crystal heating, which is especially apparent at high drive voltages. It is important to allow the crystal to thermally equilibrate before performing amplitude measurements]. In order for amplitude measurements to be

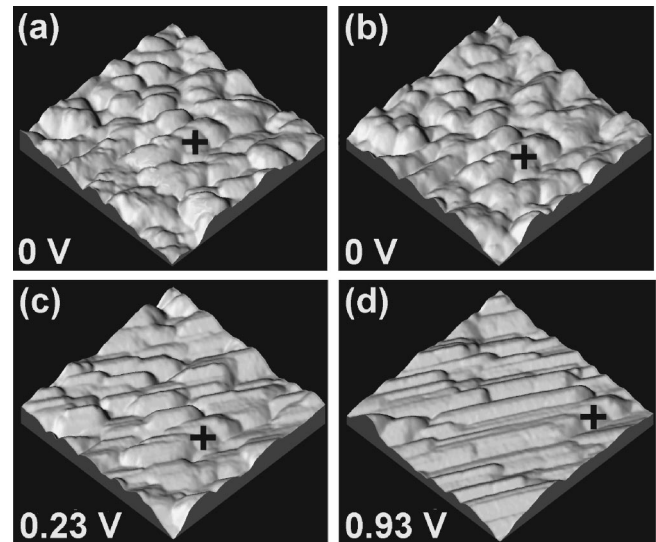


FIG. 4. A series of four  $266\text{ nm}\times 266\text{ nm}$  images from a large data set. The black cross marks the same feature in all images. The vertical scale is the same as the lateral scale. Images (a) and (b) show the stationary surface before and after, respectively, a long period of oscillation. Images (c) and (d) show the same region during oscillation at two different drive voltages,  $0.23$  and  $0.93\text{ V}$ , respectively.

precise, it is important that the surface does not change during the rapid oscillations of the quartz. This is a strict requirement due to the huge accelerations experienced on the surface, which may readily be estimated to be over  $50$  million meters per second squared, or  $5$  million  $g$ 's! In the extreme case, an ever changing and shifting surface would render the amplitude measurements impossible. The high degree of similarity between images (a) and (b) indicates that our images display the roughness of the solid copper surface evaporated onto the quartz. The movement of any loose surface material plays a minimal role. In fact, one may readily identify the detailed outlines of several prominent structures in images of the oscillating surface, as seen in images (c) and (d). Comparing the length  $L_1$  of a given feature before and after oscillation, one typically finds agreement to within  $1\text{ nm}$ . Occasional changes in the resolution of an STM tip can easily account for this small uncertainty. Apart from reproducibility, the requirements for an asperity to be useful for amplitude measurements are that it must protrude sharply from the surface and rise above surrounding features. Low lying features and those with neighbors of similar height appear either covered over or smeared together as the oscillation amplitude increases.

Having established our method for measuring amplitudes, we proceed to analyze the resonance of quartz using an approach that will be familiar to all those who have studied the classic driven harmonic oscillator problem.<sup>18</sup> Resonances of an oscillatory system are often characterized by their resonance curves, which display the amplitude of the steady state motion versus the drive frequency for a fixed drive level. The amplitude reaches a maximum at the resonant frequency, and the width of the peak is related to the quality factor  $Q$  of the system. In Fig. 5, we present a set of resonance curves constructed from our images using a range of peak drive voltages  $0.23\text{--}0.93\text{ V}$ . For all curves, the reso-

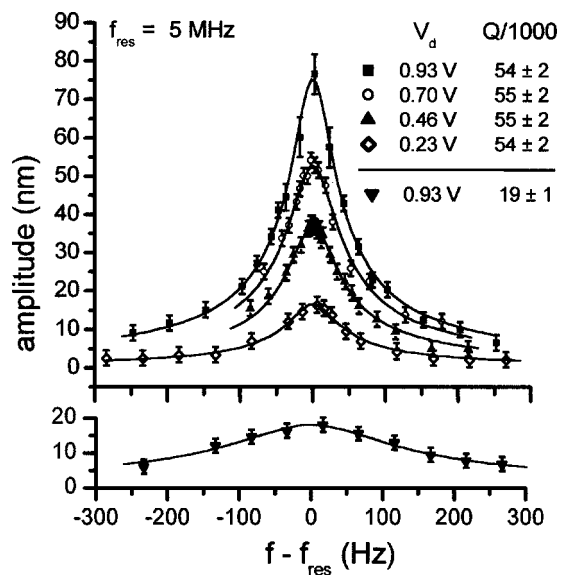


FIG. 5. Resonance curves for a 5 MHz AT-cut quartz disk oscillating in the fundamental transverse shear mode for a range of drive voltages and quality factors. The amplitude is measured at the center of the disk, where it is a maximum. These curves allow determination of the resonant frequency.

nant frequency was very close to 5 MHz, and we have displayed the frequency relative to resonance on the X axis. The drive voltage and quality factor for each data set were determined using the aforementioned electrical techniques. To guide the eye, the data for each curve were fitted to the classical expression for the amplitude of a sinusoidally driven mass subject to linear restoring and damping forces. However, we did not use the fit parameters or peak widths in our analysis.<sup>22</sup> Comparison of our data with a detailed theory for quartz oscillations is to follow below. It should be noted that the measured resonant frequency is not strictly that of the quartz disk by itself, but is influenced by the electrical circuit in which the crystal is an element. While the influence of the circuit on the resonant frequency is relatively minor, its influence on  $Q$  can be large. For instance, the curve in the bottom of Fig. 5 exhibits a much reduced value of  $Q$  from the top four curves. This was produced by removing one ground wire connection.

The information in Fig. 5 may be summarized qualitatively by remarking that the amplitude of oscillation increases with both drive voltage and  $Q$ . We analyze these relationships quantitatively in Figs. 6 and 7 by plotting the maximum amplitude at resonance versus drive voltage and  $Q$ , respectively, with the other variable held constant. Returning to basic driven oscillator theory, we develop a simple prediction. For high  $Q$  systems ( $Q > 100$ ), the maximum amplitude at resonance is closely approximated by  $A_{\text{res}} = Q * A_0$ , where  $A_{\text{res}}$  is the amplitude at resonance for a given sinusoidal drive level, and  $A_0$  is the static displacement for the corresponding static drive level (zero drive frequency).<sup>11</sup> In our case, the static displacement is expected to be proportional to the applied voltage  $V_d$  (for small displacements). Therefore, we have

$$A_{\text{res}} = C * Q * V_d, \quad (2)$$

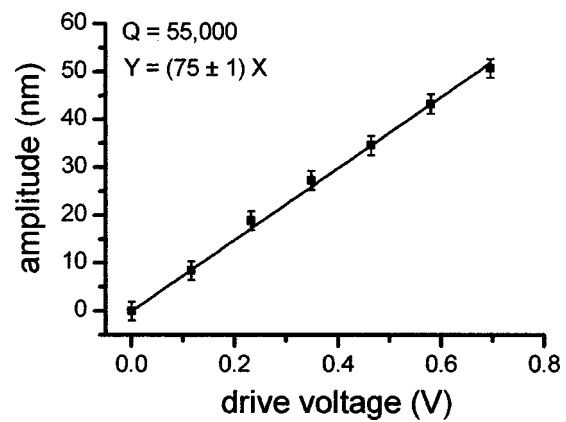


FIG. 6. A plot of the amplitude at resonance vs peak drive voltage.

where  $C$  is a proportionality constant. The data in Figs. 6 and 7 support the conclusion that the amplitude is proportional to both drive voltage and  $Q$ , and allow us to determine the value of  $C$ . This value is then compared to that obtained in a recent theoretical calculation by Kanazawa.<sup>12</sup>

Figure 6 shows a plot of the amplitude at resonance versus drive voltage for a  $Q$  of  $55\,000 \pm 2000$ . The resonant frequency was determined directly from the images, although determining the frequency of the voltage minimum across the crystal-inductor combination brought us to within 20 Hz of true resonance. The plot clearly demonstrates that the resonant amplitude is directly proportional to the drive voltage. It is significant that the points of nonzero amplitude extrapolate directly to the origin as the drive voltage is decreased to zero. In particular, this shows that one may accurately predict the length  $L_1$  of a feature by extrapolating its elongated length  $L_2$  to zero drive voltage, providing strong evidence that our technique measures amplitudes correctly. By Eq. (2), we see that the slope of the fitted line is  $C * Q$ . Dividing the slope of 75 nm/V by  $Q$ , we find that  $C = 1.4 \pm 0.1$  pm/V.

Figure 7 shows a plot of the amplitude at resonance versus  $Q/1000$  for a peak drive voltage of 0.93 V. We obtain a good fit to a line through the origin, indicating that the amplitude is proportional to  $Q$ . However, the data point at the lowest value of  $Q$  lies off the line. The value of  $Q$  for this point was obtained by disconnecting a ground wire, whereas

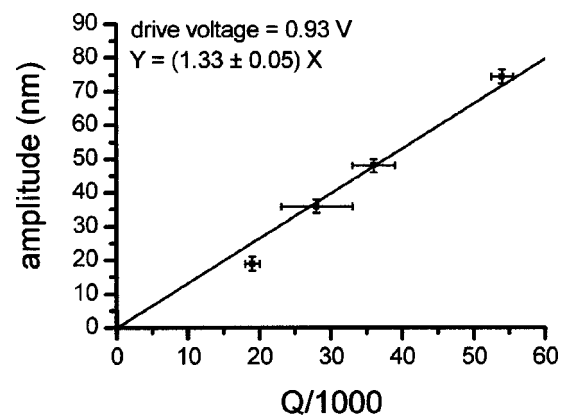


FIG. 7. A plot of the amplitude at resonance vs  $Q/1000$ .

the variation in  $Q$  for the other three points is due to slight changes in the mounting of the crystal. The disconnected wire subjects the lowest data point to inaccuracy in the drive voltage. By Eq. (2), the slope of the fitted line is  $C \cdot V_d \cdot 1000$ . Using the slope of 1.33 nm and the drive voltage, we find that  $C = 1.4 \pm 0.1$  pm/V, in agreement with the result of Fig. 6.

#### IV. DISCUSSION

The amplitude of oscillation of a quartz resonator was recently investigated by Kanazawa.<sup>12</sup> We may compare our results to Kanazawa's theory for bare quartz since the metal films we have deposited on our samples are very thin. Using a physical model for a bare AT-cut 5 MHz quartz resonator, Kanazawa calculates an amplitude of 133 nm using a peak drive voltage of 1.0 V and a  $Q$  of 100 000. Just as with basic oscillator theory, the amplitude is expected to be proportional to drive voltage and  $Q$  in Kanazawa's model

$$A_{av} = C_{av} \cdot Q \cdot V. \quad (3)$$

Using the above equation and the stated results, the theoretical value of  $C_{av}$  is found to be 1.3 pm/V. Within the model, the amplitude is interpreted as the average amplitude across the crystal. This is expected to be about one half the maximum amplitude at the center of the crystal, in view of the approximately Gaussian amplitude distribution.<sup>3</sup> The theoretical value  $C_{av}$  is thus expected to be half that of our experimental value  $C$ . We find, however, that the two values are equal. Therefore, we see that agreement between experiment and theory is within a factor of 2. We note that using very simple arguments, Martin and Hager conclude that  $C_{av}$  is equal to the piezoelectric strain coefficient for AT-cut quartz, known to be 3.1 pm/V.<sup>3</sup> According to our measurements, this approach overestimates the amplitude by more than a factor of 4.

#### V. SUMMARY

In conclusion, we find that our measurements of the amplitude of oscillation of a transverse shear quartz resonator agree with theoretical calculations to within a factor of 2. The results may be summarized as follows:

$$\text{Theory: } A_{av} = 1.3 \cdot Q \cdot V_d \\ (\text{average, } = 1/2 \text{ maximum}),$$

$$\text{Expt: } A_{\max} = (1.4 \pm 0.1) \cdot Q \cdot V_d \quad (\text{maximum})$$

where  $A$  is in pm and  $V_d$  is the peak drive voltage in volts. We expect these results will be very useful to other researchers, who may use them to better characterize the surface amplitude and velocity distributions in experiments with AT-cut quartz resonators as long as the  $Q$  of the system and the drive voltage are determined.

#### ACKNOWLEDGMENTS

The authors would like to thank Chris Daly for his role in developing the experimental apparatus, and Kay Kanazawa for helpful discussions. This work was supported by funding from the AFOSR (49620-98-1-0201) and the NSF (CMS9634374, DMR9896280).

- <sup>1</sup>C. Lu and A. W. Czanderna, *Applications of Piezoelectric Quartz Crystal Microbalances*, Methods and Phenomena, edited by S. P. Wolsky and A. W. Czanderna (Elsevier, New York, 1984), Vol. 7.
- <sup>2</sup>*Interactions of Acoustic Waves with Thin Films and Interfaces*, Faraday Discussions (Royal Society of Chemistry, Cambridge, UK, 1997), Vol. 107.
- <sup>3</sup>B. Martin and H. Hager, *J. Appl. Phys.* **65**, 2630 (1989).
- <sup>4</sup>G. Sauerbrey, *Proc. Annu. Freq. Control Symp.* **18**, 63 (1967).
- <sup>5</sup>For a complete review of the various techniques for measuring quartz vibrations, see H. Bahadur and R. Parshad, *Phys. Acoust.* **16**, 37 (1982).
- <sup>6</sup>R. Gerdes and C. Wagner, *Appl. Phys. Lett.* **18**, 39 (1971).
- <sup>7</sup>H. Bahadur and R. Parshad, *Indian J. Pure Appl. Phys.* **18**, 905 (1980).
- <sup>8</sup>H. Bahadur and R. Parshad, *IEEE Trans. Sonics Ultrason.* **SU-27**, 303 (1980).
- <sup>9</sup>W. Spencer, *Phys. Acoust.* **5**, 111 (1968).
- <sup>10</sup>L. Wimmer, S. Hertl, J. Hemetsberger, and E. Benes, *Rev. Sci. Instrum.* **55**, 605 (1984).
- <sup>11</sup>A. P. French, *Vibrations and Waves* (Norton, New York, 1966), p. 91.
- <sup>12</sup>K. Kanazawa, *Faraday Discuss.* **107**, 77 (1997).
- <sup>13</sup>McAllister Technical Services, Coeur d'Alene, ID (1-800-445-3688).
- <sup>14</sup>Digital Instruments, Santa Barbara, CA, (1-800-873-9750), *NanoScope II* electronics.
- <sup>15</sup>Stanford Research Systems, Sunnyvale, CA (408-744-9040), Model DS-345 function generator.
- <sup>16</sup>M. E. Frerking, *Crystal Oscillator Design and Temperature Compensation* (Van Nostrand Reinhold, New York, 1978), p. 85.
- <sup>17</sup>R. J. Matthys, *Crystal Oscillator Circuits* (Wiley, New York, 1983), pp. 69–77.
- <sup>18</sup>J. B. Marion and S. T. Thornton, *Classical Dynamics of Particles and Systems*, 3rd ed., (Harcourt Brace Jovanovich, New York, 1988), p. 116.
- <sup>19</sup>E. Watts, J. Krim, and A. Widom, *Phys. Rev. B* **41**, 3466 (1990).
- <sup>20</sup>We used a standard analog oscilloscope and  $\times 10$  probes to measure voltages. In general, one needs to be careful not to disturb a circuit due to capacitive loading when probing voltages at high frequency. In our case, the STM tip signal served as a sensitive check of whether the probes disturb the drive voltage,  $Q$ , or resonant frequency. By connecting and disconnecting the probes while observing the tip signal, we found that the probes do not disturb the circuit. (The STM tip, with its high gain current-to-voltage amplifier, acted as an antenna, producing an ac signal proportional to that on the electrode facing the tip).
- <sup>21</sup>Advanced Surface Microscopy, Indianapolis, IN (1-800-374-8557), Model HD-750 calibration standard.
- <sup>22</sup>Our resonance peaks are slightly narrowed due to the difficulty of keeping the drive voltage exactly constant while changing the drive frequency. Essentially, this is because the crystal's impedance changes rapidly with frequency near resonance, reaching a minimum at  $f_{res}$ . We held the voltage  $V_1$  in Fig. 2 constant by adjusting the output voltage of the generator. However, the increasing crystal impedance reduced  $V_2$  such that the drive voltage was reduced on either side of resonance. The resulting narrowed peak widths give artificially high values for  $Q$ . We therefore report only electrically measured  $Q$  values, which have been checked for accuracy by the technique in Ref. 19.